12. McFee R, Parungao A: An orthogonal lead system for spatial electrocardiography. Am Heart J **62:** 93, 1961
13. Draper HW, Peffer CJ, Stallmann FW, Littmann C, Pipberger HV: Corrected orthogonal electrocardiograms and vectorcardiograms in 510 normal men (Frank lead system). Circulation **30:** 853, 1964
14. Pipberger HV, Goldman MJ, Littmann D, Murphy FP, Cosma J, Snyder JR: Correlations of the orthogonal electrocardiogram and vectorcardiogram with constitutional variables in 518 normal men. Circulation **35:** 536, 1967
15. Borun ER, Chapman JM, Massey FJ: Electrocardiographic data recorded with Frank leads in subjects without cardiac disease and in subjects with left ventricular overload. Am J Cardiol **18:** 656, 1966
16. Borun ER, Chapman JM, Massey FJ Jr: Computer analysis of Frank lead electrocardiographic data recorded in an epidemiologic study. Am J Cardiol **18:** 664, 1966
17. Bristow JD: A study of the normal Frank vectorcardiogram. Am Heart J **61:** 242, 1961
18. McCall B, Wallace AG, Estes EH Jr: Characteristics of the normal vectorcardiograms. A study using the Frank lead system. Am J Cardiol **10:** 514, 1962
19. Forkner CE Jr, Hugenholtz PG, Levine HD: The vectorcardiogram in normal young adults, Frank lead system. Am Heart J **62:** 237, 1961
20. Liebman J, Romberg HC, Agusti R, Downs TD: The Frank QRS vectorcardiogram in the premature infant. *In* Vectorcardiography 1965, edited by Hoffman I, Taymor R. Amsterdam, North-Holland Publishing Co, 1966, p 256
21. Hugenholtz PG, Liebman J: The orthogonal vectorcardiogram in 100 normal children (Frank system). Circulation **26:** 891, 1962
22. Namin EP, Arcilla RA, D'Cruz IA: Evolution of the Frank vectorcardiogram in normal infants. Am J Cardiol **13:** 757, 1964
23. Namin EP, D'Cruz IA: Vectorcardiogram in normal children. Br Heart J **26:** 689, 1964
24. Khoury GH, Fowler RS: Normal Frank vectorcardiograms in infancy and childhood. Br Heart J **29:** 563, 1967
25. Gamboa R, White N: The corrected orthogonal electrocardiogram in normal children. McFee-Parungao lead system. Am Heart J **75:** 449, 1968
26. Borun ER, Sapin SO, Goldberg SJ: Scalar amplitude measurements of data recorded with cube and Frank leads from normal children. Circulation **39:** 859, 1969
27. Paul MH, Muster AJ, Kardotzke ML: The normal QRS vectorcardiogram in infancy and childhood: An exploration of correlated structure based upon inflection point sampling. *In* Vectorcardiography 1965, edited by Hoffman I, Taymor R. Amsterdam, North-Holland Publishing Co, 1966, p 285
28. Ellison RC, Restieaux NJ: Vectorcardiography in Congenital Heart Disease. Philadelphia, W. B. Saunders Co, 1972
29. Ainger LE, Dixon PR: The Frank vectorcardiogram of the normal four-month old infant. Am J Cardiol **29:** 693, 1972
30. Ainger LE, Dixon PR: The Frank vectorcardiogram of the normal newborn. Am J Cardiol **29:** 686, 1972
31. Guller B, Berg KLM, Weidman WH, O'Brien PC, Dushane JW, Smith RE: Computer interpretation of Frank vectorcardiogram in normal newborns: Identification of right ventricular dominance patterns. J Electrocardiol **5:** 307, 1972
32. Guller B, O'Brien PC, Smith RE, Weidman WH, Dushane JW: Computer interpretation of Frank vectorcardiogram in normal infants: Longitudinal and cross sectional observations from birth to two years of age. J Electrocardiol **9:** 201, 1975
33. Guller B, O'Brien PC, Smith RE, Weidman WH: Computer interpretation of right ventricular hypertrophy from Frank vectorcardiograms in children with congenital heart disease. Mayo Clin Proc **49:** 466, 1974
34. Blumenschein SD, Barr RC, Spach MS, Geritzler RC: Quantitative Frank vectorcardiograms of normal children and in comparison to those of patients with atrial defects. Am Heart J **83:** 332, 1972
35. Lee MH, Liebman J, Mackay W: Orthogonal electrocardiograph correlative study of 100 children with pure cardiac defects. *In* Vectorcardiography 2, edited by Hoffman I, Hamby I. Amsterdam, North-Holland Publishing Co, 1976, p 181
36. Liebman J, Downs TD, Priede A: The Frank and McFee vectorcardiogram in normal children. A detailed quantitative analysis of 105 children between the ages of two and 19 years. *In* Vectorcardiography 2, edited by Hoffman I, Hamby, I. Amsterdam, North-Holland Publishing Co, 1971, p 483
37. Liebman J, Lee MH, Rao PS, Mackay W: Quantitation of the normal Frank and McFee-Parungao orthogonal electrocardiogram in the adolescent. Circulation **48:** 735, 1973
38. Downs TD,Liebman J, Agusti R, Romberg HC: The statistical treatment of angular data in vectorcardiography. *In* Vectorcardiography 1965, edited by Hoffman I, Taymor R. Amsterdam, North-Holland Publishing Co, 1966, p 272
39. Liebman J, Downs TD, Agusti R, Romberg HC: The statistical treatment of angular data in vectorcardiography. (abstr) Am J Cardiol **17:** 129, 1966
40. Downs TD, Liebman J: Statistical methods for vectorcardiographic directions. IEEE Trans Biomed Eng **16:** 87, 1969

Sampling Rates Required for Digital Recording of Intracellular and Extracellular Cardiac Potentials

ROGER C. BARR, PH.D., AND MADISON S. SPACH, M.D.

SUMMARY **Electrocardiograms and cardiac electrograms now frequently are measured for both clinical and experimental purposes by direct digital sampling, with no recording of the signal in analog form. This study examined the question of what sampling rates were required to measure accurately the continuous waveforms from the digital samples. Body surface waveforms and intracellular and extracellular waveforms measured directly from cardiac tissues were evaluated. Cardiac measurements included waveforms from the atrium, ventricle, atrioventricular transmission system and individual Purkinje strands. Sampling rates as high as 15,000 samples/sec were required to record accurately extracellular waveforms of the ventricular conduction system. Decreasing sampling rates were required as the recording site shifted through the ventricle to the body surface, where sampling rates as high as 1500 samples/sec were necessary.**

ELECTROCARDIOGRAMS AND CARDIAC ELECTROGRAMS now frequently are recorded by immediately converting the potentials from analog to digital form, and retaining only the digital samples (no analog recording). Despite the increased use of this form of recording, an essential question remains unanswered: What minimum sampling rates are required to retain all of the information in the original waveforms? In this study we directly examined the effect of different sampling rates by repeatedly reconstructing the same cardiac waveforms from different sets of samples resulting from different sampling rates. Since waveforms now are recorded digitally from the atrium, ventricle, atrioventricular (A-V) transmission system, and individual Purkinje strands, numerous cardiac electrical waveforms

From the Departments of Biomedical Engineering and Pediatrics, Duke University Medical Center, Durham, North Carolina.

Supported in part by USPHS grants HL 11307, HL 5716, HL 07101, and a grant from the National Foundation March of Dimes.

Address for reprints: Roger C. Barr, Ph.D., Box 3305, Duke Medical Center, Durham, North Carolina 27710.

Received June 16, 1976; revision accepted July 27, 1976.

ranging from intracellular action potentials to body surface electrocardiograms were examined in this way.

An important characteristic of cardiac waveforms which must be considered in judging the quality of the waveforms reconstructed from different sampling rates is that cardiac waveforms often include notches or other irregularities of relatively high frequency and low amplitude. Such notches are known to be physiologically significant. For example, in body surface recordings, the notches sometimes occur because of myocardial infarction[1] or hypertrophy,[2] and in the conduction system the notches can be associated with the asynchronous activity of separate strands.[3] Because of the significance of the notches, the minimum sampling rate was defined as the lowest rate which allowed the complete analog waveform, continuous in time, to be reproduced within the noise level from the retained digital samples. This definition had the advantages of being consistent with the usual practice of interpreting cardiac waveforms by direct visual inspection; the definition also allowed a straightforward evaluation of how well each sampling rate reproduced a particular waveform.

The evaluation of different sampling rates was based on waveform reconstruction, rather than on a frequency analysis, even though it is well known that the sampling rate required for a given waveform is closely related to the frequency content of the waveform. A waveform reconstruction procedure, instead of a frequency analysis procedure, was used for the following reasons. The theory of sampling shows that if a function of time contains no frequencies higher than W Hz, then it is completely determined by giving its value at a series of points spaced $1/(2W)$ seconds apart.[4] If such a waveform is sampled at this rate or a higher rate, the theory shows that the waveform can be reconstructed by interpolation using sine functions. Precise application of this relationship to cardiac waveforms is not possible, however, since cardiac waveforms do not have all the characteristics required by the theory, and because of the difficulties in practice of identifying the upper frequency limit W.

Although the theoretical relationship remains valid in an approximate sense, it is difficult to apply it accurately to real waveforms because of the significance of the small notches in cardiac waveforms. Since such notches are of relatively high frequency and low amplitude compared to other features of the waveforms, they produce an effect on the frequency spectrum of the waveform which overlaps with the effects of low amplitude noise. Consequently, it is not possible, except by arbitrary choice, to identify from the measured frequency spectra of cardiac waveforms an upper frequency limit, W, that includes only the physiologically significant waveform information and excludes only noise. Additionally, until now the only cardiac waveforms subject to frequency analysis have been waveforms recorded from the body surface,[5-8] but waveforms from the heart itself have not been analyzed.

Methods

Recording and Selection of Waveforms to be Analyzed

To record extracellular potentials from the heart and body surfaces, AC amplifiers were used that had a flat frequency response between 0.1 and 35,000 Hz.* Intracellular action potentials of the dog ventricular conduction system were recorded with a Keithley DC amplifier. The extracellular and intracellular electrodes and the recording system used for the *in vitro* conduction system measurements have been described in detail previously.[9] The extracellular electrodes were flexible tungsten wire 50μ in diameter. The microelectrodes for intracellular measurements had a tip resistance varying from 5 to 15 megohms. The deleterious capacitance effects between the microelectrode and the bathing solution were reduced to a minimum by a system which neutralized the input capacitance.[10] For all measurements, the overall system rise time (10–90%) for the intracellular and extracellular recording systems was measured to be less than 20μ sec.[9] Plunge electrodes with recording points 1 to 2 mm apart were used for acute open chest and chronic intact dog intramural ventricular measurements of unipolar and bipolar waveforms.[11] The body surface measurements were made as unipolar leads with all potentials recorded in reference to Wilson's central terminal.

All analog signals were sampled in real time by an analog-to-digital converter at sampling rates as high as 50,000 samples per second. A PDP-11/20 computer system[12] stored the data and displayed the waveforms immediately on a Tektronix 4002 display unit. The waveforms were inspected and, if they were free of artifact, recorded on a digital tape. Simultaneously, the waveforms were displayed on a Tektronix 565 oscilloscope, and they were photographed with a Grass camera. The waveforms recorded photographically from the oscilloscope were considered to be accurate and were used as the standard against which the reconstructed digital waveforms were compared.

Waveforms were selected for analysis that were recorded from: 1) the body surface of humans and dogs with normal and abnormal excitation and repolarization events;[13-16] 2) the atrial epicardium of the dog; 3) the epicardial surface of the ventricular muscle of the dog;[17] 4) the ventricular muscle of the dog as measured with intramural plunge electrodes;[11] 5) the left ventricular conduction system of the dog.[3, 18] For the measurements from the heart, intracellular action potentials and extracellular unipolar and bipolar waveforms were included. From all of the above, about 1000 waveforms were selected initially using visual inspection, and of these about 100 were analyzed fully using the quantitative procedure below.

Analysis Procedure to Determine the Minimum Sampling Rate

The first step of the analysis was the collection of waveforms from different locations on the body surface and in the heart, as described above. Each of these waveforms had been sampled originally at a high enough rate so that a plot of the successive samples, connected by straight lines, looked identical to the original analog waveform displayed on the oscilloscope.

Second, samples were eliminated from the original sampled waveform, thereby producing a sparsely sampled

*These amplifiers were designed by Dr. J. Mailen Kootsey, Department of Physiology, Duke University Medical Center. The complete circuit diagram will be supplied upon request.

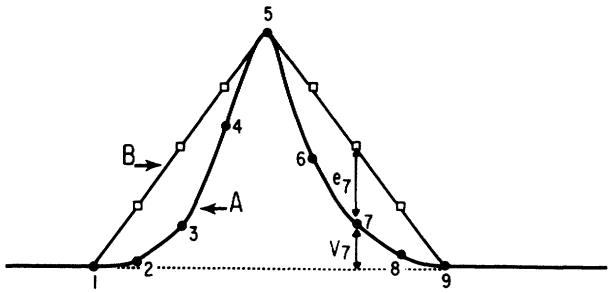

FIGURE 1. *Method of calculation. The heavy solid line (A) represents the original hypothetical waveform, and the black solid dots numbered 1 to 9 represent the original set of samples. Time is plotted on the abcissa and voltage on the ordinate.*

waveform. One sparse waveform was produced by taking every other sample of the original; a second sparse waveform was produced by taking every fourth sample of the original, etc.

Third, values for all the missing samples in each of the sparse waveforms, i.e., those samples that had been eliminated in step two, were reconstructed from the remaining samples. For each sparsely sampled waveform, reconstructions were made using three methods: 1) a linear (L) interpolation from adjacent samples, 2) a quadratic (Q) interpolation from the preceding and two following samples, or 3) a sine x/x (S) interpolation based on sampling theory.[4] The L and Q interpolation methods were included since these methods are widely used and easy to apply; these methods consist of interpolation between samples using straight lines (L) or simple curves (Q). The S method required much more computation; however, it is theoretically superior in that under certain restrictive conditions[4] S interpolation reproduces the original waveform exactly.

Fourth, each of the reconstructed waveforms was compared both visually and quantitatively to the corresponding original waveform. If the reconstructed waveform was close to the original one, it was concluded that the lower sampling rate represented by the remaining samples in the sparsely sampled waveform was sufficient. For quantitative comparison of the original and reconstructed waveforms, the "mean error" was defined as the mean squared difference between the entire original waveform and the entire reconstructed waveform divided by the mean squared value of the original waveform. The resulting fraction was multiplied by 100 so that mean error was expressed as a percentage.

An example of the calculation procedure is shown in figure 1. In the example, a hypothetical original waveform

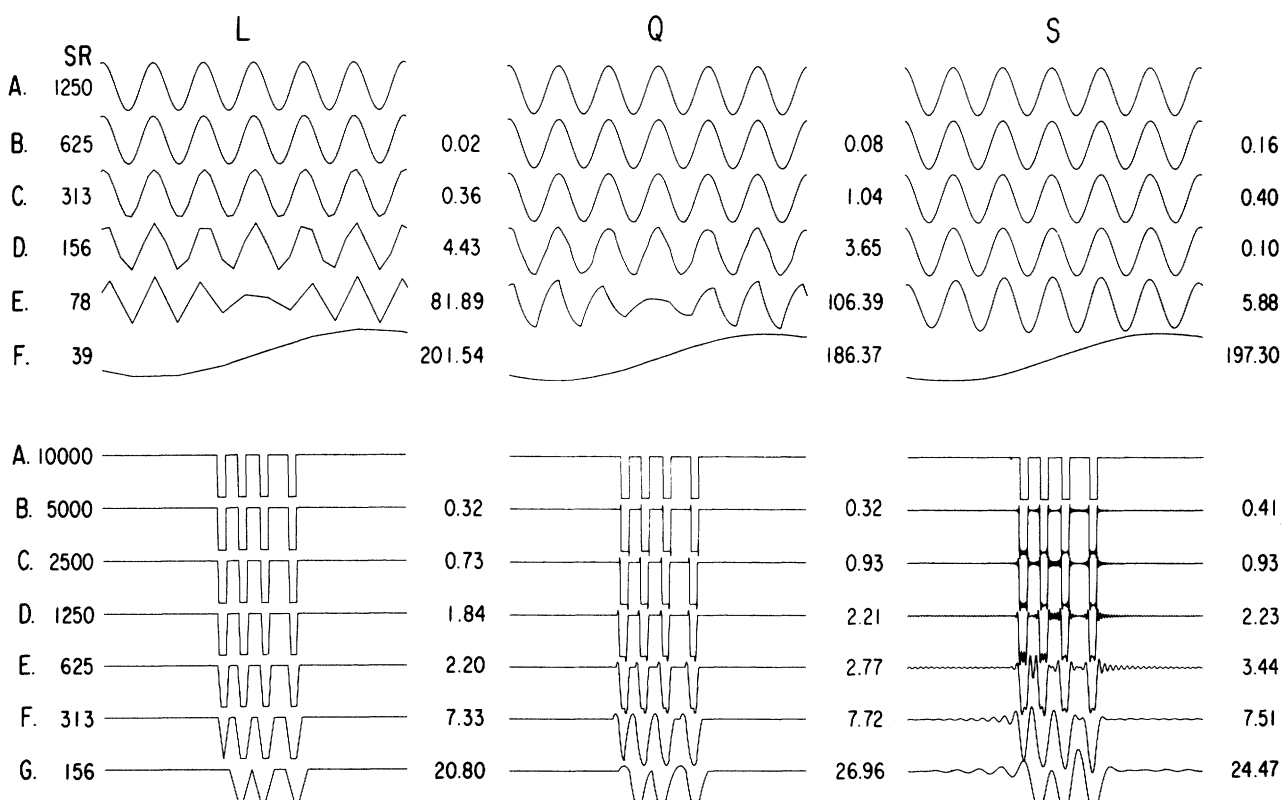

FIGURE 2. *Example of reconstruction of waveforms for different interpolation methods. A 35 Hz sine wave (top half) and a burst of 100 Hz square waves (bottom half) were reconstructed from different sampling rates. Columns 1, 2, and 3 (L, Q, and S) show reconstruction of the waveforms using linear, quadratic, and sine x/x forms of interpolation. The rows show the result when the sampling rate (SR) was reduced stepwise by a factor of 2. The number to the right of each waveform is the mean error of that waveform compared to the original one in row A; for example, the error percentage of the sine wave when sampled at 156 samples per second and reconstructed with linear interpolation is 4.43%. Waveforms in this and the following figures were drawn automatically by a Houston plotter.*

was drawn as a dark line, A, and the original set of samples at a fast rate was symbolized by the dark circles, numbered 1 to 9. (In the real waveforms, this original set of samples was always taken at a high enough rate so that straight lines drawn between the samples made a waveform identical to that of the analog tracing displayed on the oscilloscope.) The example was to illustrate the test of whether samples 1, 5, and 9 alone were sufficient to describe the waveform. To make this test, samples 2, 3, 4, and 6, 7, 8 were ignored. That is, the sparsely sampled waveform included only samples 1, 5, and 9. Next, a reconstructed waveform, B, was produced from samples 1, 5, and 9 by joining these samples with straight lines, i.e., linear interpolation. Reconstructed values for samples 2, 3, 4 and 6, 7, 8 were the values of the reconstructed waveform at the times of the original samples. The reconstructed sample values were symbolized by open squares.

The original waveform and the reconstructed waveform were compared by examining the difference in voltage at the time of each sample. For example, at point 7, the original voltage is drawn and marked by V_7, and the difference (i.e., error) is marked e_7. The difference, along with the differences at all other sample times, was used to determine the mean error, as defined above, between the original and reconstructed waveforms.

Different interpolation methods were used to reconstruct the waveforms since significantly different waveforms could result from the use of different interpolation methods. Two examples of this are shown in figure 2. The top half of figure 2 shows reconstructions for different sampling rates of a 35 Hz sine wave. In the first column, all of the original sample values were reconstructed using L interpolation. Columns 2 and 3 were reconstructed using Q and S interpolation. The top row (A) shows the same sine wave in all three columns. The waveform in row A was measured using a sampling rate of 1250 samples per second. This waveform was identical to the analog record. Rows B through F show the same waveform as reconstructed after some samples were deleted. Every other sample was deleted in row B, three of every four in row C, etc., thus resulting in the effective sampling rate for each row shown in column SR.

This example shows that L interpolation (first column) produced visible flattening of the sine wave peaks at 313 samples per second (and at slower sampling rates). With Q interpolation (middle column), the waveform was unchanged at 313 samples per second, but was distorted at sampling rates of 156 and below. With S interpolation (third column), the waveform remained undistorted when the sampling rate was reduced to 156 and even to 78 samples per second. Note that only S interpolation produced a good reconstruction at 78 samples per second, even though this sampling rate is more than twice the sine wave's frequency of 35 Hz.

The bottom half of figure 2 shows a burst of four 100 Hz square waves originally measured at 10,000 samples per second. With the square waves, L interpolation produced waveforms with practically no distortion at 2500 samples per second, and still provided a good reproduction of the original waveform at 1250 samples per second. In contrast, Q interpolation produced visible overshoots near the corners of the square waves at sampling rates as high as 5000 per second, and S interpolation produced extensive ringing at this and lower sampling rates. Note that S interpolation produced the worst results for the square wave, in contrast to the results for the sine wave where S interpolation produced the best results. Because of the highly variable shape of cardiac waveforms as related to sine, square, or other test waveforms, we knew of no way to determine in advance which of the three methods of interpolation would be the best. Therefore, each of the cardiac waveforms was reconstructed by all three methods to determine if any one method was systematically better than the others.

Results

An example of the analysis of a precordial body surface waveform recorded from a normal newborn baby is shown in figure 3. Row A shows the original waveform at a sampling rate of 1667 samples per second. This waveform was identical to the analog one. In row A, note the low-amplitude rapid deflections during QRS at the time indicated by the arrow. It is evident that these deflections were not due to noise since they recur on the next beat. Rows B through G show the same waveform reconstructed with progressively lower sampling rates. At a rate of 834 samples per second (row B), the rapid deflections still were present; however, at 417 samples per second there were not as many rapid deflections. At 208 samples per second the entire waveform was smoothed somewhat, and the rapid deflections at the time of the arrow no longer were visible. Note that the mean error was only 0.71% even at 208 samples per second.

Waveforms were analyzed from adults with normal hearts, left ventricular hypertrophy, and myocardial infarcts. These waveforms required lower sampling rates than did the waveforms from babies. Examples of six waveforms

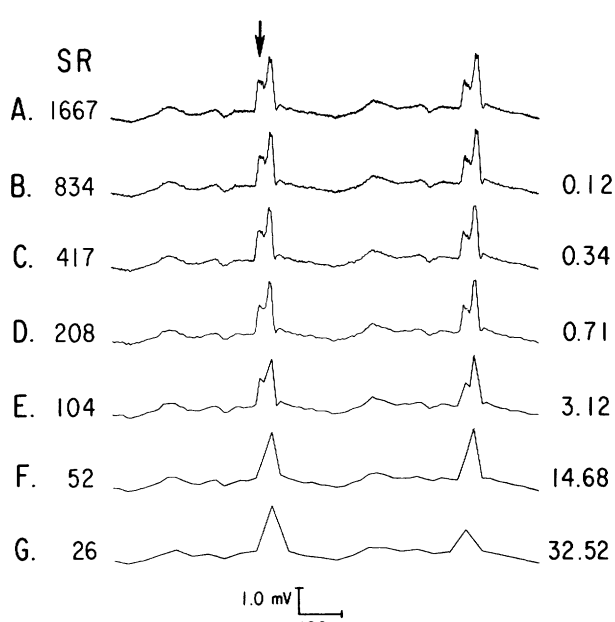

FIGURE 3. *Body surface waveform from a baby. The unipolar waveform was recorded from the right parasternal area in the fourth intercostal space in a normal 3-day-old baby. The same format as figure 2 is used, except that only reconstruction by L interpolation is shown.*

from adults are shown in figure 4 with panels A through F ordered by increasing complexity of the wave shape. The waveforms were measured from a variety of sites on the anterior chest. An original sampling rate of 1000 samples per second was adequate for all the waveforms, and the waveform measured at this rate is shown at the top of each panel. At 500 samples per second, the waveforms of all panels were almost unchanged. At 250 samples per second, visible differences near the peaks and in the notches were present between the reconstructed waveform and the original one, but the differences were small. At 125 samples per second, some waveform notches were no longer visible (note panels C and F especially), and the peaks of the waveforms were changed substantially. At 62 and 31 samples per second, even the gross waveform features were changed. Note that the mean error value at the boundary between acceptable and unacceptable waveforms, as judged visually, is approximately 0.5% for all panels.

Sampling rates similar to those required for newborn babies also were required to record accurately precordial body surface waveforms in newborn puppies. In figure 5, the original waveform, recorded at 3125 samples per second, is shown at the top of all three columns. The waveform reconstructed from 1563 samples per second was almost unchanged from the original waveform, but visible differences existed at 781 samples per second, particularly with L inter-

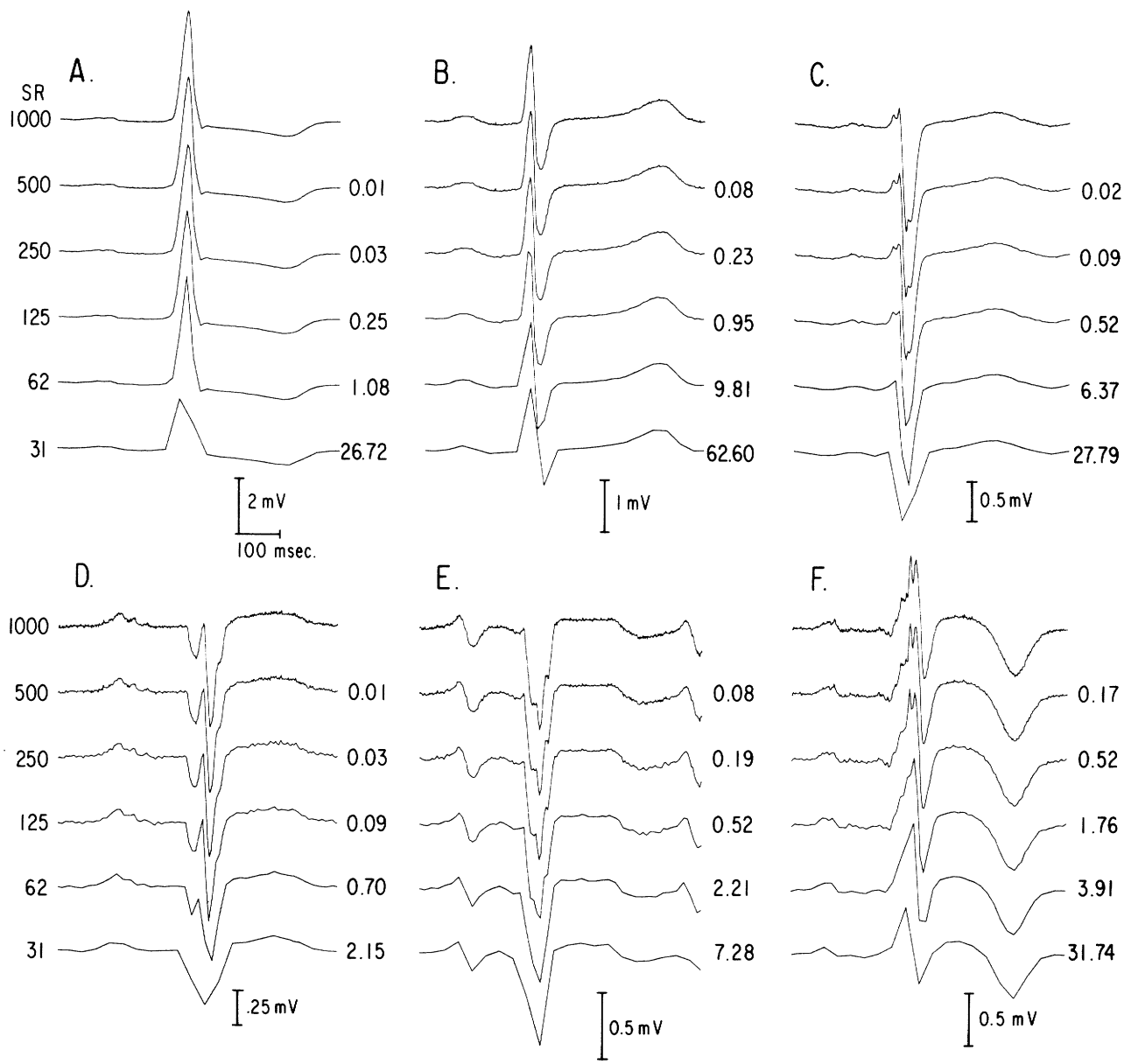

FIGURE 4. *Body surface waveforms from adults. Each of the six panels shows a waveform measured from a different person. The format for each panel is the same as that of figure 3. All reconstructions are by L interpolation. The diagnosis, age in years, and recording position as related to the standard precordial leads for each subject was:* A) *aortic stenosis, age 53, 3 cm below* V_5; B) *normal, age 50, 6 cm below* V_3; C) *normal, age 51,* V_2; D) *anterior lateral infarct, age 52, 3 cm below* V_5; E) *Diaphragmatic infarct, age 60, 3 cm below* V_1; F) *anterior infarct, age 64, 6 cm below* V_4.

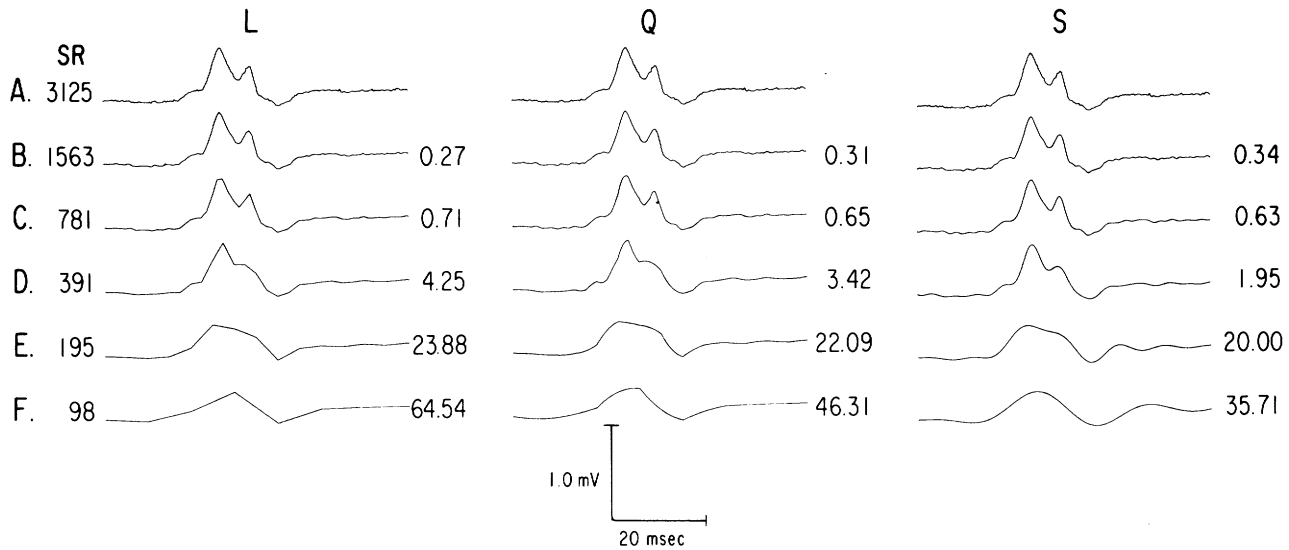

FIGURE 5. *QRS body surface waveform recorded from a one-day-old puppy. The waveform was recorded in the right parasternal area in the fourth interspace. In rows B through F, the three columns of the figure show reconstructions of the waveform using the three interpolation methods. Note that differences exist between the waveforms produced by a sampling rate (SR) of 781 and those at higher rates (row C compared to row A or B in each column). At a SR of 391, the second hump is greatly diminished in all cases, and the basic waveform shape is lost at a SR of 195 (rows D and E of all columns).*

polation, with a corresponding error of about 0.70%. Gross reduction of the amplitude of the second peak was evident using all methods of interpolation at 391 samples per second, and at 195 samples per second the major waveform features no longer were recognizable.

Considerably higher sampling rates were required for extracellular waveforms of the ventricular conduction system of a dog, as shown in figure 6. The unipolar waveform shown was recorded *in vitro* at 42,000 samples per second with a 50μ extracellular electrode placed on the proximal portion of the posterior extension of the main left bundle branch.[3] This extension contained multiple separate but closely spaced conducting strands which excited slightly asynchronously, thereby producing overlapping effects in the surrounding extracellular space. These overlapping effects produced a complicated polyphasic waveform. Note that in rapid portions of the waveform the voltage rose to a maximum and then declined to a minimum in less than one msec.

Only minimal change occurred in the waveform at a rate of 21,000 samples per second. However, at 10,500 samples per second, some truncation of the peaks and valleys occurred before the major downward deflection. At 5,250 samples per second, the signal was grossly distorted, and the mean error rose to 27.8%. At 2,125 samples per second, the original signal was lost almost totally.

The waveforms of the preceding figures were measured at the extremes of location of the recording point with respect to the heart, i.e., from the body surface and from the ventricular conduction system. These waveforms required the lowest and highest sampling rates of all the extracellular waveforms examined. An analysis of additional waveforms requiring intermediate minimum sampling rates is shown in figure 7. The extracellular recording sites for these waveforms shifted from unipolar recordings of the ventricular conduction system (P_1 and P_2) to bipolar and unipolar recordings in the left ventricular wall of the dog (B and U) to body surface precordial tracings in two normal adults, age 50 and 69 years (Q_1 and Q_2). The data in figure 7 are shown as a plot of mean error versus sampling rate for the six waveforms. Note the log scale on both axes of the graph. Other unipolar and bipolar waveforms (not shown in figure 7) from the ventricular and atrial epicardium also gave results similar to the intramural results of lines U and B.

Two important results were evident from the results of figure 7. The first was that the required sampling rate was extremely variable depending on the source of the waveform, e.g., approximately 30 times the sampling rate re-

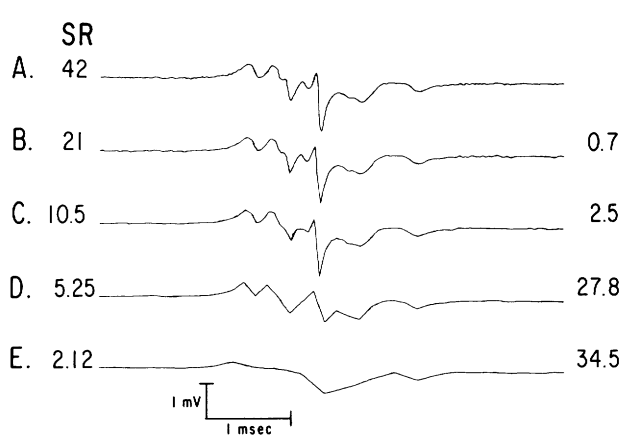

FIGURE 6. *Analysis of an extracellular waveform recorded from the left ventricular conduction system of a dog. The sampling rate for each row is the value in column SR times 1000. All reconstructions are by Q interpolation. Note that this waveform had considerably faster components than those shown in figure 5 for the body surface, and that gross distortion of this waveform occurred at sampling rates as high as 5,250 samples per second.*

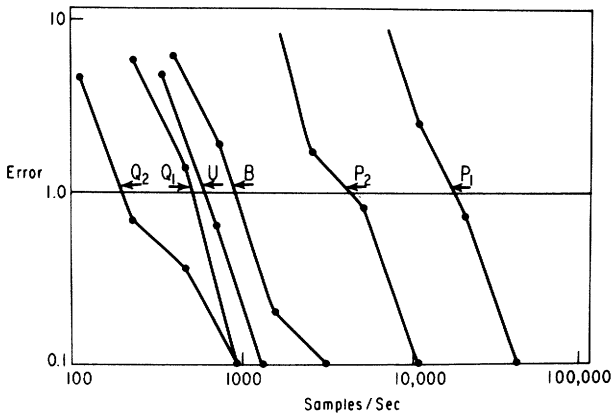

FIGURE 7. *Analysis of extracellular waveforms recorded from in the heart and on the body surface. Each line of the plot corresponds to a different waveform, as follows: Q_1, Q_2 are two body surface waveforms (adult human), U and B are unipolar and bipolar intramural waveforms (dog), and P_1 and P_2 are two waveforms from the conduction system (dog). Note the log plot on both the sampling rate axis and the error axis.*

quired for the body surface waveforms was necessary for the conduction system waveforms, with other waveforms requiring intermediate minimum sampling rates. The second result was the rapid degradation of each waveform once the sampling rate was reduced below a critical level. Note that a change in the mean error from 0.1 to 1.0, a factor of 10 change, required a change in the sampling rate of approximately a factor of 4. This relationship was about the same for all waveforms as was evident from the similar slopes of all the plots in the figure.

Sampling rates required to measure intracellular action potentials were determined using the same protocol followed for extracellular waveforms. Figure 8, top, shows a waveform recorded from a Purkinje strand on the left ventricular endocardium of a dog, at 10,000 samples per second. For comparison, an extracellular waveform with Purkinje and muscle deflections also measured from the ventricular endocardium is shown in figure 8, bottom. The intracellular waveform remained unchanged when the sampling rate was reduced to 5000 samples per second, but changes in the upstroke were visible at 2500 samples per second, in all three columns. Flaws were seen clearly in the waveforms reconstructed from 1250 samples per second. Even with these errors, the mean error remained well under 1% for L and Q interpolation. The small mean error was because of the long intracellular plateau phase which was accurately reproduced from the lower sampling rates.

The possibility that one interpolation method was systematically superior to another was examined both visually and quantitatively. The extracellular as well as intracellular waveforms of figure 8 show examples of the variability of

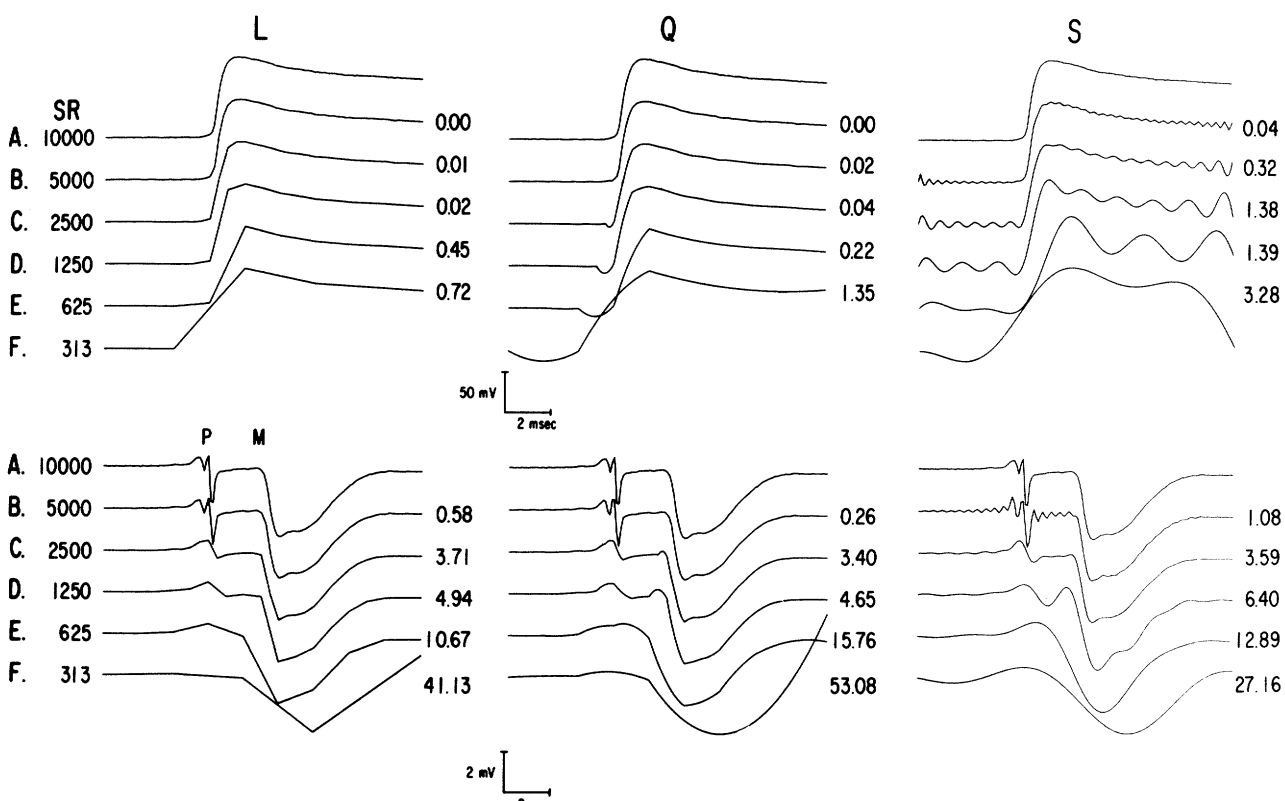

FIGURE 8. *Analysis of an intracellular action potential. The top panels show an action potential measured from ventricular muscle on the endocardial surface (dog). For comparison at the same rates the bottom panels show an extracellular recording from the ventricular endocardium of the same dog with Purkinje (P) and muscle (M) deflections. Note that the Purkinje deflection on the extracellular waveform is truncated slightly at the peaks even at the maximum rate of 10,000 samples per second.*

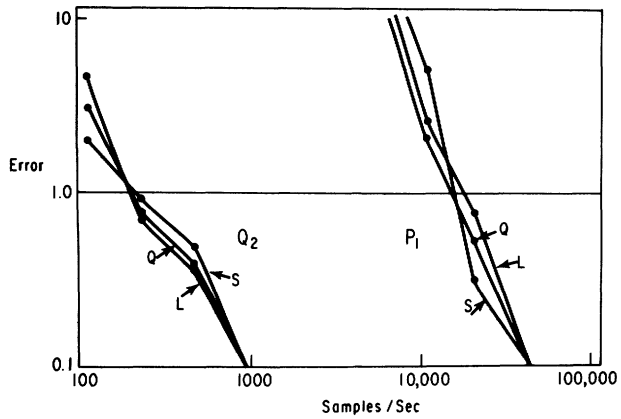

FIGURE 9. *Comparison of different methods of interpolation. Mean error plots are shown for L, Q, and S interpolation. Note that at any error level the difference between signals Q_2 (normal adult) and P_1 (extracellular recording from Purkinje strand) along the sampling rate axis was much greater than the differences among the L, Q, and S methods for a given signal. Note also that neither the L, Q, nor S method consistently had the lowest error.*

waveforms reconstructed with different interpolation methods, as seen by visual comparison. Quantitative comparison was done by plotting mean error versus sampling rate for L, Q, and S reconstructions of a given waveform. Figure 9 shows the results of such a procedure for a body surface and a conduction system extracellular waveform. Although the sampling rates required for the two waveforms are considerably different, for either waveform the L, Q, and S error plots overlap. Plots of this kind always showed that the wave shape itself, which was strongly associated with the type of measurement and location of the electrode, was a much greater factor in determining the minimum required sampling rate than was the interpolation method.

Discussion

Sources of Small Deflections in the Waveforms

Since cardiac waveforms tend to be quite irregular in shape, a fixed sampling rate which is adequate for the entire waveform effectively is determined by the sampling rate necessary to measure the most rapid waveform deflections. These deflections are often small notches which occur during cardiac depolarization. For strands of the ventricular conduction system, one source of these irregularities is the overlapping effects of different strands.[3] For ventricular muscle as a whole, the irregularities are much slower, and arise from the overlapping effects of different portions of the ventricles which are simultaneously active.[11]

Body surface waveforms from humans have been extensively studied with respect to waveform irregularities. Langer and Geselowitz[7] associated notching, slurring, and beading with fibrosis of the myocardium following infarction. Pipberger and Carter[19] performed a computerized count of waveform irregularities in vectorcardiograms from patients with both normal and abnormal hearts, and pointed out that QRS deformities sometimes occurred in abnormal frequencies in both hypertrophy and conduction defects. Reynolds et al.[20] emphasized the importance of notches as opposed to slurs as evidence of cardiac disease. Selvester et al.[21] developed specific criteria for interpreting VCGs on the basis of their irregular features, and emphasized the importance of high-frequency response in oscilloscopic VCG records. Flowers et al.[2] pointed out that ventricular enlargement without scarring produced high-frequency components indistinguishable from those produced by infarction, but went on to show that, when infarction was present, its site could be associated with the occurrence of notching in specific ECG leads.[22] All of the above studies have associated the high-frequency notches in the waveforms with superimposed effects from different cardiac sources, as opposed to the possibility of very complicated waveforms arising from a single cardiac source.

Minimum Sampling Rates for Extracellular Waveforms

The objective of this study was to determine sampling rates which were sufficient to retain all of the information present in the original waveforms. Because numerous studies, cited above, have shown that waveform notches and slurs contain substantial information, the sampling rates were required to be high enough to record the entire waveform, including the short low amplitude features, but excluding noise. Visual comparison of waveforms that were reconstructed from different sampling rates showed that the maximum mean error that could be attributed to noise was less than one percent. The results presented in figure 7 showed that if a mean error of this size was allowed, the minimum sampling rate for body surface waveforms was 500 samples per second; for waveforms from ventricular muscle 1000 samples per second; and for waveforms from the ventricular conduction system, 15,000 samples per second.

For a number of waveforms that were examined, however, additional considerations indicated that sampling rates higher than those given above were required. One consideration was that visible errors in the reconstructed waveforms often became significant at error levels well below 1%. For this reason, body surface waveforms from babies required a sampling rate of 834 samples per second (fig. 3), and those from newborn puppies required rates as high as 1563 samples per second. Another consideration was that plots of the size of the mean error versus the sampling rate (fig. 7) showed that the error increased rapidly as the sampling rate became marginal; this result implied that sampling rates that are twice or more the minimum rates are highly desirable to allow for accurate measurement of unexpectedly complicated waveforms.

Two further factors that would lead to sampling rates higher than the minimum rates also are worth noting. First, sampling rates that are several times the minimum rates required to reconstruct the waveform are frequently advantageous in subsequent waveform analysis; the redundant samples lessen any effects of noise and may simplify data processing procedures. Second, waveforms quite possibly occur that have more rapid deflections or notches than those of the waveforms we analyzed. These waveforms would therefore require higher sampling rates. In this regard, Franke and associates[23] reported frequency components up to 3000 Hz from body surface measurements on selected leads from patients with ischemic heart disease.

Intracellular Action Potentials

A sampling rate of 5000 samples per second was sufficient to reproduce all of the intracellular action potentials examined in this study. All action potentials studied were measured from the ventricular epicardium, endocardium, or conduction system *in vitro*. This sampling rate was sufficient to eliminate visible artifact in the upstroke as seen on a time scale showing the complete action potential waveform. A higher sampling rate might be required if detailed features of the upstroke were of interest; however, these detailed features were not examined in this study. The fact that the minimum sampling rates required for intracellular waveforms were lower than those required for extracellular waveforms just outside Purkinje strands is not surprising since the shape of the extracellular waveforms is similar to the shape of the second derivative of the intracellular one.[18]

Comparison of Methods of Interpolation

At the beginning of the investigation, it was anticipated that the results for intracellular or extracellular waveforms might be systematically dependent on the method of interpolation. An analysis of artifically generated waveforms showed that for special cases such as sine waves this was the case (fig. 2). However, no systematic superiority of one interpolation method over another was observed for cardiac waveforms, although varying kinds of artifact were produced at marginal sampling rates depending on the interpolation method used. In general, L interpolation produced sharp corners, Q interpolation produced overshoots, and S interpolation produced ringing. All of these effects can be seen, for example, in the intracellular and extracellular waveforms from Purkinje and muscle shown in figure 8. Since only three interpolation methods were tested, out of the large number of interpolation and filtering methods that have been proposed and used in many scientific contexts, the results do not demonstrate that some other interpolation method that was not tested would not have been superior to all of the ones that were. However, it is worth noting that more complicated interpolation methods are used primarily in situations where each sample value is known to a high accuracy; it is difficult to take advantage of such methods in interpolating experimentally measured cardiac waveforms because the measurement noise is inevitably of comparable size to the smallest waveform features of interest. The results therefore indicate that for cardiac waveforms the overall number of samples that must be retained to record the waveform may be more readily reduced by using a less complicated form of interpolation together with some form of data compression[24, 25] (i.e., a variable sampling rate that retains fewer samples during periods of slower potential variation) than by using a more complicated interpolation method and a slower fixed sampling rate.

Significance of the Question of Minimum Sampling Rates

From a clinical viewpoint, the results indicate that the use of a sampling rate that is too low for the specific recording site results in degradation of the waveform in a manner that can lead to errors in timing measurements and misinterpretation of the wave shape. From a practical viewpoint, the increasing cost of the equipment associated with increasing sampling rates currently limits the number of channels of data that can be simultaneously sampled. This is so since it is necessary to have data sampling and data storage devices capable of dealing with the aggregate rate of all channels, i.e., the sampling rate per channel times the number of channels being recorded. From a theoretical viewpoint, the sampling rate can be viewed as a measure of the rate at which the signal is conveying information to the observer. Thereby, these results show quantitatively that as signals closer and closer to individual heart fibers are observed, information about what is happening is received at a higher and higher rate.

References

1. Langner PH Jr: Further studies in high fidelity electrocardiography: Myocardial infarction. Circulation **8:** 905, 1953
2. Flowers NC, Horan LG, Thomas JR, Tolleson WJ: The anatomic basis for high-frequency components in the electrocardiogram. Circulation **39:** 531, 1969
3. Spach MS, Barr RC, Johnson EA, Kootsey JM: Cardiac extracellular potentials: Analysis of complex waveforms about the Purkinje networks in dogs. Circ Res **33:** 465, 1973
4. Shannon CE: Communication in the presence of noise. Proc of the IRE **37:** 10, 1949
5. Reid WD, Caldwell SH: Research in electrocardiography. Ann Intern Med **7:** 369, 1933
6. Scher AM, Young AC: Frequency analysis of the electrocardiogram. Circ Res **8:** 344, 1960
7. Langner PH Jr, Geselowitz DB: Characteristics of the frequency spectrum in the normal electrocardiogram and in subjects following myocardial infarction. Circ Res **8:** 577, 1960
8. Golden DP Jr, Wolthuis RA, Hoffler GW: A spectral analysis of the normal resting electrocardiogram. IEEE Trans BME **20:** 366, 1973
9. Spach MS, Barr RC, Serwer GA, Johnson EA, Kootsey JM: Collision of excitation waves in the dog Purkinje system: Extracellular identification. Circ Res **29:** 499, 1971
10. Kootsey JM, Johnson EA: Buffer amplifier with femtofarad input capacity using operational amplifiers. IEEE Trans BME **20:** 389, 1973
11. Spach MS, Barr RC: Ventricular intramural and epicardial potential distributions during ventricular activation and repolarization in the intact dog. Circ Res **37:** 243, 1975
12. Barr RC, Herman-Giddens GS, Spach MS, Warren RB, Gallie TM: The design of a real-time computer system for examining the electrical activity of the heart. Comput Biomed Res **9:** 445, 1976
13. Benson DW, Barr RC, Spach MS, Walston A II: A clinically usable isopotential body surface mapping system. Circulation **49, 50** (suppl III): III-96, 1974
14. Walston A II, Spach MS, Barr RC, Gallagher JJ: Prediction of site of preexcitation with isopotential body surface maps in patients undergoing surgery for WPW syndrome. Circulation **49, 50** (suppl III): III-249, 1974
15. Edwards SB, Walston A II, Barr RC, Spach MS: Isopotential body surface maps in atrial and ventricular arrythmias. Circulation **49, 50** (suppl III): III-81, 1974
16. Ramsey M III, Barr RC, Spach MS: Relation of ventricular epicardial and body surface potential distributions in the intact dog (normal QRS-T). Circulation **49, 50** (suppl III): III-97, 1974
17. Spach MS, Barr RC: Analysis of ventricular activation and repolarization by means of intramural and epicardial potential distributions for ectopic beats in the intact dog. Circ Res **37:** 830, 1975
18. Spach MS, Barr RC, Serwer GA, Kootsey JM, Johnson EA: Extracellular potentials related to intracellular action potentials in the dog Purkinje system. Circ Res **30:** 505, 1972
19. Pipberger HV, Carter TN: Analysis of the normal and abnormal vectorcardiogram in its own reference frame. Circulation **25:** 827, 1962
20. Reynolds EW Jr, Muller BF, Anderson GJ, Muller BT: High-frequency components in the electrocardiogram. A comparative study of normals and patients with myocardial disease. Circulation **35:** 195, 1967
21. Selvester RH, Rubin HB, Hamlin JA, Pote WW: New quantitative vectorcardiographic criteria for the detection of unsuspected myocardial infarction in diabetics. Am Heart J **75:** 335, 1968
22. Flowers NC, Horan LG, Tolleson WJ, Thomas JR: Localization of the site of myocardial scarring in man by high-frequency components. Circulation **40:** 927, 1969
23. Franke EK, Braunstein JR, Zellner DC: Study of high frequency components in the electrocardiogram by power spectrum analysis. Circ Res **10:** 870, 1962
24. Gardenhire LW: Data redundancy reduction for biomedical telemetry. *In* Biomedical Telemetry, chapter 11. Edited by CA Caceres. Academic Press, 1965
25. Dower GE: Compression and transmission. Biomed Eng **9:** 296, 1974